JGR Atmospheres

RESEARCH ARTICLE
10.1029/2025JD044757

Special Collection:
TEMPO Data Products, Science, and Applications

Tropospheric NO_2 Patterns in Eastern Canada Using the First Year of TEMPO Observations

Tsz Kin Siu[1], Daniel L. Goldberg[2], Gaige H. Kerr[2], Lulu Chen[2], M. Omar Nawaz[2,3], Rachel Y.-W. Chang[4], and Kelvin C. Fong[1,2]

[1]Department of Earth and Environmental Sciences, Dalhousie University, Halifax, Nova Scotia, Canada, [2]Department of Environmental and Occupational Health, Milken Institute School of Public Health, George Washington University, Washington, DC, USA, [3]School of Earth and Environmental Science, Cardiff University, Cardiff, UK, [4]Department of Physics and Atmospheric Science, Dalhousie University, Halifax, Nova Scotia, Canada

Abstract The Tropospheric Emissions: Monitoring of Pollution (TEMPO) instrument enables an unprecedented assessment of diurnal and community-scale variations in tropospheric nitrogen dioxide (NO_2) across North America. This study presents the first exploratory analysis of NO_2 patterns in eastern Canada, including Ontario, Quebec, and the Atlantic provinces, using TEMPO observations. We analyzed TEMPO data (V03) gridded at 0.02° × 0.02° from September 2023 to August 2024 and compared it with the Tropospheric Monitoring Instrument (TROPOMI) and surface-level measurements from Canadian national regulatory monitors. With the hourly resolution of TEMPO, we observed diurnal trends and hotspots that were not recognized by once-per-day TROPOMI measurements and pinpointed undermonitored areas. NO_2 in eastern Canada's eight major metropolitan areas, ports, and industrial cities similarly peaked in early morning and declined in later hours. Still, TEMPO detected variations in their hours of peaks and spikes, seasonal, and weekday-weekend distributions. In Atlantic Canada, correlations between TEMPO and TROPOMI column densities, as well as column-surface alignments, were lower (Spearman's $\rho = 0.41$–0.53) compared to the Quebec City-Windsor Corridor (Spearman's $\rho = 0.81$–0.90), primarily due to a wider dynamic range of pollution in the latter region. The two regions' TEMPO-TROPOMI mean absolute differences were 19.3% and 17.1%, respectively. Temporal variations (e.g., a later weekday morning peak in Ontario cities) and TEMPO's identification of additional undermonitored hotspots provide insights into air quality control planning. Our findings motivate future research using multiyear TEMPO data to investigate atmospheric NO_2 sources, transport, exposure, and associated population health impacts in Canada.

Plain Language Summary Nitrogen dioxide (NO_2) is an air pollutant primarily associated with anthropogenic emissions and poses a significant health burden. A new satellite instrument, Tropospheric Emissions: Monitoring of Pollution (TEMPO), monitors NO_2 pollution in eastern Canada covering more hours during daytime. Using TEMPO's first-year observations from September 2023 to August 2024, this study explores NO_2 spatiotemporal patterns in Ontario, Quebec, and the Atlantic provinces. High NO_2 concentrated in large metropolitan areas (e.g., Toronto, Montreal), industrial cities (e.g., Windsor, Sarnia, Saint John), and port communities (e.g., Halifax, Quebec City). TEMPO identified additional municipalities with high NO_2 pollution previously unobserved in suburban and remote areas. We observed annual, seasonal, weekday-weekend, and diurnal NO_2 characteristics, which might be attributed to local traffic, industry, and wind-driven transport. These patterns can provide implications for air pollution control. Our findings also motivate future research on applying TEMPO for studying NO_2 exposure and its impacts in eastern Canada.

Key Points:

- TEMPO observed diurnal NO_2 variations in eight major polluted areas in eastern Canada, generally with a morning peak and mid-day decline
- TEMPO identified previously unrecognized NO_2 hotspots and undermonitored suburban communities
- TEMPO-TROPOMI and column-surface correlations were weaker in Atlantic Canada than in southern Ontario and Quebec due to a smaller dynamic range

Supporting Information:

Supporting Information may be found in the online version of this article.

Correspondence to:
T. K. Siu,
ts577891@dal.ca

Citation:
Siu, T. K., Goldberg, D. L., Kerr, G. H., Chen, L., Nawaz, M. O., Chang, R. Y.-W., & Fong, K. C. (2025). Tropospheric NO_2 patterns in eastern Canada using the first year of TEMPO observations. *Journal of Geophysical Research: Atmospheres*, *130*, e2025JD044757. https://doi.org/10.1029/2025JD044757

Received 30 JUN 2025
Accepted 28 NOV 2025

Author Contributions:
Conceptualization: Tsz Kin Siu, Kelvin C. Fong
Data curation: Tsz Kin Siu
Formal analysis: Tsz Kin Siu
Funding acquisition: Kelvin C. Fong
Investigation: Tsz Kin Siu
Methodology: Tsz Kin Siu
Project administration: Kelvin C. Fong

© 2025. The Author(s).
This is an open access article under the terms of the Creative Commons Attribution-NonCommercial-NoDerivs License, which permits use and distribution in any medium, provided the original work is properly cited, the use is non-commercial and no modifications or adaptations are made.

1. Introduction

Satellite remote sensing has played a vital role in air pollution monitoring in recent decades (Holloway et al., 2021, 2025). Spaceborne sensors passively detect solar radiances reflected or backscattered through the atmosphere. Identification of pollutants is based on the unique spectral signatures of gaseous molecules and aerosols (Hoff & Christopher, 2009). Through differential optical absorption spectroscopy, a slant column density (SCD) is retrieved, representing the total integrated amount of a trace gas along the entire effective light path from the sun to the detector between the top of atmosphere and the surface. Vertical column density (VCD) representing ambient air pollution directly above the grid location is obtained from the transformation of SCD. This involves computing an air mass factor (AMF) that considers altitude-dependent scattering (Nowlan et al., 2025;

Resources: Rachel Y.-W. Chang, Kelvin C. Fong
Software: Tsz Kin Siu
Supervision: Kelvin C. Fong
Validation: Tsz Kin Siu
Visualization: Tsz Kin Siu
Writing – original draft: Tsz Kin Siu
Writing – review & editing: Daniel L. Goldberg, Gaige H. Kerr, Lulu Chen, M. Omar Nawaz, Rachel Y.-W. Chang, Kelvin C. Fong

Palmer et al., 2001), followed by a stratosphere-troposphere separation process that first estimates *a priori* tropospheric enhancements from independent instruments and then applies spatial filtering based on stratospheric and tropospheric AMF ratios (Geddes et al., 2018; González Abad et al., 2024).

Tropospheric Emissions: Monitoring of Pollution (TEMPO) is a satellite instrument launched in April 2023 monitoring a variety of trace gas pollutants over the continental United States (U.S.), northern Mexico, and southern Canada. Regular observations started August 2023. TEMPO operates with a geostationary orbit that provides approximately hourly available data, compared to the approximately once-per-day revisit cycle of sun-synchronous satellites (Chance et al., 2019; Naeger et al., 2021), thus enabling a more comprehensive understanding of the temporal evolution of atmospheric pollutants during daytime. Comparing hourly column and in situ surface-level measurements can also inform how well TEMPO measurements infer surface air quality distributions. Furthermore, TEMPO's spatial resolution attains 2 km × 4.5 km at the center of its field of regard (FoR) (33.7°N, 91.7°W) (Naeger et al., 2024), which is finer than its predecessor instruments, such as the ozone monitoring instrument (OMI) and the Tropospheric Monitoring Instrument (TROPOMI). Higher resolution observations enable more detailed assessments of spatial variability at the community level.

During TEMPO's 20-month baseline operation phase (Phase *E*) from 2023 October to 2025 June, it measured tropospheric and stratospheric nitrogen dioxide (NO_2), total column ozone (O_3), and total column formaldehyde (HCHO) (Liu et al., 2025; Naeger et al., 2024). In this study, we are interested in tropospheric NO_2 VCD, which is associated predominantly with anthropogenic sources, such as traffic and industrial emissions at the ground level, as well as natural sources like soil microbial activity and lightning. NO_2 is one of the criteria air contaminants in Canada (Statistics Canada, 2012), with well-studied acute and chronic impacts on human health (Brook et al., 2007; Manisalidis et al., 2020; Parajuli et al., 2021). Exposure to NO_2 is associated with respiratory and lung diseases, particularly pediatric asthma (Achakulwisut et al., 2019; Anenberg et al., 2022) and chronic obstructive pulmonary disease (Gan et al., 2013), and increases the risks of all-cause hospitalization and mortality (Mills et al., 2015).

TEMPO addresses gaps in surface air pollution monitoring, providing an avenue toward understanding spatio-temporal NO_2 patterns across all communities. Eastern Canada, including Ontario (ON), Quebec (QC), and the Atlantic provinces of Nova Scotia (NS), New Brunswick (NB), Newfoundland and Labrador (NL), and Prince Edward Island (PEI), has sparse surface NO_2 monitoring. NO_2 pollution in eastern Canada is attributed to several factors. First, more than half of the population and around 75% of manufacturing activities in Canada are concentrated in the Quebec City-Windsor (QW) Corridor along the southern edges of ON and QC, with major cities including Windsor, London, Hamilton, Kitchener, Toronto, Ottawa, Montreal, and Quebec City (Lévesque, 2010). High commuting demand leads to the highest transportation volume nationally along the corridor. In recent years, population growth has driven urban expansion that increases anthropogenic emissions. Second, the St. Lawrence River connecting the Atlantic and the Great Lakes areas is a busy marine logistics and transportation route (Meng & Comer, 2022). Third, transboundary air pollution from the Northeastern United States can affect air quality in eastern Canada given midlatitude westerlies (Environment and Climate Change Canada (ECCC) and U.S. Environmental Protection Agency (EPA), 2024; Stevens et al., 2024).

We examined the first year of TEMPO tropospheric NO_2 VCD data covering eastern Canada from 1 September 2023 to 31 August 2024 and addressed the following objectives: (a) mapping spatial NO_2 distribution to identify highly polluted communities; (b) visualizing daytime hourly NO_2 trends among the most polluted communities, with seasonal and weekday-weekend variations; (c) comparing TEMPO and TROPOMI NO_2 hotspots for surface monitoring gap implications; and (d) evaluating TEMPO with TROPOMI and surface-level regulatory monitoring data.

2. Data and Methods

2.1. TEMPO Tropospheric NO_2 Products

We accessed TEMPO Version 03 tropospheric NO_2 VCD from the National Aeronautics and Space Administration (NASA)'s Earthdata Search platform (NASA, 2024), noting that this version recently completed its provisional validation. At high latitudes, pixel resolution becomes coarser due to a larger view-angle distortion between the Earth's surface and the satellite's nadir. For convenience and consistency, we directly used Level 3

data for analysis. Level 3 is the extension of Level 2, which is geo-referenced, calibrated, quality-assessed, retrieved in standard units, and with pixels regridded from the native spatial resolution across nine granules to 0.02° × 0.02° (around 2 km × 2 km) (Chance et al., 2013; Zoogman et al., 2017). The resampling is based on area-weighted averaging covering all pixels in a complete scan (González Abad et al., 2024; Naeger et al., 2024).

For quality control, we followed the TEMPO Science Team's recommendations on masking tropospheric NO_2 VCD to minimize uncertainties (González Abad et al., 2024). Using ancillary data, we retained only pixels flagged with good quality (i.e., "main_QA_flag" = 0, effective cloud fraction below 20%, and snow-ice fraction below 5%). These filters account for the removal of outliers, extreme viewing geometry (solar zenith angle (SZA) between incident sunlight and vertical direction above the local grid and viewing zenith angle (VZA) between the local grid position and the satellite's line of sight), shadowing effects, bright surfaces, and successful AMF calculation from *a priori* geophysical information (González Abad et al., 2024). TEMPO tropospheric NO_2 VCD is expressed as the number of molecules per square centimeters (molec/cm^2). Still, good-quality retrievals may contain negative values based on the allowable range of SCD (González Abad et al., 2024).

2.2. Extracting Temporal Aggregates of TEMPO NO_2

We aggregated TEMPO tropospheric NO_2 VCD averages using different temporal grouping dimensions to assess spatiotemporal variabilities. These attributes included (a) year (from 1 September 2023 to 31 August 2024), (b) seasons (fall: September–November 2023; winter: December 2023–February 2024; spring: March–May 2024; summer: June–August 2024), (c) weekdays (Monday–Friday) and weekends (Saturday–Sunday), and (d) daytime hourly intervals. Besides single-dimension aggregation, we stratified weekday and weekend averages by adding seasons as the secondary dimension, and similarly, splitting hourly averages specific to seasons and days of week. To reduce striping on these annual and seasonal mean-aggregated images (Nowlan et al., 2025) for better visual interpretation, we have applied a Gaussian filter, which performed horizontal and vertical convolutions sequentially with Gaussian kernels (Pan & Chang, 1992).

Each granule's scan takes around 6–7 min (Naeger et al., 2024). Atlantic Canada is situated in the first two (easternmost) granules, while the QW Corridor overlaps mainly with the third and fourth granules. We adjusted the binning of daytime hours for all observations accordingly based on the scanning start time from the first granule (González Abad et al., 2024). Scans starting after the 47th and 34th min are assigned to the next hour for Atlantic Canada and the QW Corridor, respectively. Also, we accounted for changes in time zones for both regions during the daylight-saving period to adapt to hours in local time.

2.3. Spatiotemporal Analysis of TEMPO NO_2 at Regional and Local Scales

We first mapped and examined the annual and seasonal distributions of TEMPO tropospheric NO_2 VCD in the two regional extents (Atlantic Canada: −69.05°W to −52.05°W, 43.05°N to 51.05°N; QW Corridor: −86.05°W to −69.05°W, 41.20°N to 48.20°N). Then, we selected municipalities with high NO_2 VCD, extracting rectangles bounding their corresponding Canadian census population center boundaries for local analysis. Within each municipality, we mapped NO_2 VCD by oversampling TEMPO pixels to 0.01° × 0.01° using bilinear interpolation to align with the TROPOMI Level 3 spatial resolution. Spatial interpolation provided an approximation of NO_2 in census units smaller than a TEMPO grid at densely populated areas and increased the heterogeneity of observations to reflect NO_2 spatial gradients in smaller or medium-sized cities.

For intramunicipality analysis, we studied weekday-weekend variations and daytime hourly trends. We calculated pixelwise differences between weekday and weekend mean NO_2 VCDs (Equation 1), and between consecutive hourly mean NO_2 VCDs (i.e., first-order differences in diurnal time series) (Equation 2). The weekday-weekend contrast illustrated whether an area had higher pollution during normal working days and how large this deviation was. The hour-by-hour changes resolved the timing when pollution peaked and increased most rapidly.

Denoting V to represent temporally-averaged tropospheric NO_2 VCD, D for weekdays, E for weekends, T for any hour, for any TEMPO grid j with center's coordinates (x_j, y_j), we have

$$\Delta\left(x_j, y_j\right)\text{weekday-weekend} = \mathrm{V}_D\left(x_j, y_j\right) - \mathrm{V}_{\mathrm{E}}\left(x_j, y_j\right) \quad (1)$$

$$\Delta\left(x_j, y_j\right)\text{hour-by-hour} = \mathrm{V}_T\left(x_j, y_j\right) - \mathrm{V}_{T-1}\left(x_j, y_j\right) \quad (2)$$

Using Canadian census tract boundaries, we obtained area-weighted mean NO_2 and its differences for the weekday-weekend and hourly aggregates. To test whether these differences were statistically significant, we applied the Mann-Whitney U Test at a 5% significance level. For areas without census tracts, we used census dissemination areas (DA) instead. DA is the fundamental geographic unit for Canadian census statistics, with around 400–700 residents, while a tract (around 5,000 residents) is defined only in cities with an urban core population greater than 50,000 (Statistics Canada, 2023). Furthermore, we obtained a population-weighted average of the tract-level mean NO_2 and its difference for selected municipalities, based on the 2021 Canadian Census of Population (Statistics Canada, 2023).

2.4. Comparing TEMPO With TROPOMI and Surface-Level NO_2

To compare TEMPO with precursor satellite measurements, we accessed Level 3 TROPOMI tropospheric NO_2 VCD during the study period using Google Earth Engine (GEE) (European Space Agency, 2024), gridded at $0.01° \times 0.01°$. We used the offline version that uses more robust inputs of *a priori* information for retrievals than the near real-time data. TROPOMI Level 3 applies the same regridding logic as TEMPO, proportional to overlapping areas, using the "bin_spatial" function in HARP (data harmonization toolset for scientific earth observation data), a command line tool that enables the intercomparison of satellite data sets (S[&]T, The Netherlands, 2024). This TROPOMI data set on GEE retains pixels with a quality assurance value greater than 0.75, which corresponds to the condition that a cloud radiance fraction is below 50%, and either a snow cover fraction is below 1% or the difference between cloud pressure and surface pressure is small (van Geffen et al., 2022). For more consistent comparisons, we modified the filtering of TEMPO pixels using the "amf_cloud_fraction" variable that represents the cloud radiance fraction for calculating AMF, and adjusted the cutoffs of cloud and snow fractions to 50% and 1% accordingly. We matched and evaluated the TEMPO and TROPOMI images with an absolute scanning time difference within 15 min. Moreover, TROPOMI images with scene intersection or filtered pixels covering less than 50% of the areas of interest were discarded. For colocation, we reprojected TROPOMI pixels from $0.01° \times 0.01°$ to $0.02° \times 0.02°$ using area-weighted averaging. We refer to this data set as "spatiotemporally colocated" in later sections.

We calculated TROPOMI and TEMPO pixelwise averages, respectively, from the spatiotemporally colocated images and assessed their agreement using Pearson's (r) and Spearman's (ρ) correlation coefficients. Pearson's r is a commonly used metric, while Spearman's ρ can characterize correlations for nonnormally distributed data and is robust to outliers. Additionally, we reported the pixelwise percentage difference (PD) between TEMPO and TROPOMI tropospheric NO_2 VCDs to assess the spatial distribution of discrepancies (Equation 3). Outlier observations lower than 1×10^{14} molec/cm^2 (less than 1% of pixels) were excluded to avoid inflating the PD values.

Denoting V to represent mean tropospheric NO_2 VCD, for any colocated TEMPO and TROPOMI grid j the with center's coordinates (x_j, y_j), we define

$$\Delta_j = \left(\mathrm{V}_{\mathrm{TEMPO}}\left(x_j, y_j\right) - \mathrm{V}_{\mathrm{TROPOMI}}\left(x_j, y_j\right)\right)/\mathrm{V}_{\mathrm{TROPOMI}}\left(x_j, y_j\right) \times 100\% \quad (3)$$

The agreement between tropospheric column and surface-level NO_2 measurements is of public health and policy interests. In Canada, regulatory monitoring stations of the National Air Pollution Surveillance (NAPS) network measure near real-time air quality and upload data to AirNow (Canadian Council of Ministers of the Environment (CCME), 2019). AirNow was developed by the U.S. EPA as an automated and centralized data management system for United States and Canadian ambient pollution monitoring (White et al., 2004). We obtained hourly AirNow data for monitoring stations in the QW Corridor ($N = 41$) and Atlantic Canada ($N = 23$) from 1 September 2023 to 31 August 2024. Subsequently, we aligned the hourly intervals between TEMPO and AirNow NO_2 measurements, and bilinearly interpolated TEMPO's observations at the coordinates of these monitoring stations for colocation. Besides correlation coefficients between column and surface NO_2, we plotted their aggregated time series by months, weeks, weekdays, and daytime hours. Since surface measurements are

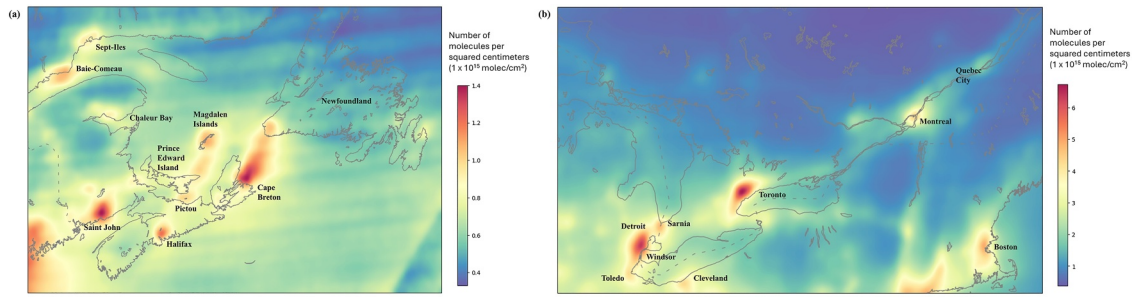

Figure 1. Spatial distribution of TEMPO (Tropospheric Emissions: Monitoring of Pollution) tropospheric nitrogen dioxide vertical column density (molec/cm^2) (from 2023 September 1 to 2024 August 31) in panel (a) Atlantic Canada and (b) the Quebec City-Windsor Corridor, aggregated as the annual average. Gaussian filter has been applied to the images for strip reduction.

expressed in parts per billion (ppb), we applied min-max normalization to scale TEMPO and AirNow observations, respectively, to a range from 0 to 1 for comparison.

2.5. Detecting Previously Unobserved and Undermonitored High-NO_2 Areas

Since TEMPO covers hours beyond TROPOMI's once-per-day local overpass time at around 13:30, we hypothesized that TEMPO could capture residential communities of high NO_2 that were unobserved by TROPOMI. We calculated the area-weighted annual mean tropospheric NO_2 VCD (September 2023–August 2024) from TEMPO and TROPOMI for each census population center in eastern Canada. Then, we ranked the population centers into percentiles by their NO_2 levels. Specifically, we extracted the population centers with TEMPO's percentile rank exceeding TROPOMI's percentile rank by 0.50 (i.e., PR_{TEMPO} (%) − $PR_{TROPOMI}$ (%) > 50%). To discern if such difference was attributable to pollution observed by TEMPO's expanded temporal coverage, or inconsistencies between TEMPO and TROPOMI, we replicated this analysis using the spatiotemporally colocated data set.

To identify communities undermonitored at the surface level, at the regional scale, we highlighted census population centers within top-decile area-weighted annual NO_2 VCD from both instruments. At intraurban scales, we calculated the bilinearly interpolated satellite measurements at each regulatory monitoring location. If these values were smaller than the 98th percentile within the municipality area, the current monitoring network could not effectively cover locations with high extremes where possible surface air quality exceedances may occur. Grids with in situ NO_2 VCD exceeding the 98th percentile and the nearest monitor having NO_2 VCD below the same percentile were considered undermonitored. Again, we repeated the top-decile and 98th-percentile mapping using the spatiotemporally colocated data set to characterize the spatial variations between TEMPO- and TROPOMI-derived pollution hotspots when time difference is minimized.

3. Results

3.1. Regional NO_2 Pollution Patterns From TEMPO

Based on TEMPO annual mean (September 2023–August 2024) tropospheric NO_2 VCD, the pixel-level maximum NO_2 in the QW Corridor (8.97×10^{15} molec/cm^2), occurring in Etobicoke in western Toronto, was more than four times higher compared to that in Atlantic Canada (2.07×10^{15} molec/cm^2), near the primary highway and railway in east Satin John. Most areas of high NO_2 VCD in the two regions were large urban centers and port communities, while rural northern parts of the domains had low NO_2 (Figure 1). Regarding seasonal variations of NO_2 for the two regions, the fall and winter means were generally higher than those in spring and summer (Figure S1 in Supporting Information S1), primarily due to the longer NO_2 lifetime during colder seasons.

In Atlantic Canada (Figure 1a), NO_2 hotspots occurred in the three most populated port municipalities (Halifax, Saint John, and Cape Breton). Notably, NO_2 in Cape Breton spread northward to the southwestern corner of Newfoundland. Likewise, we observed a dispersion of pollution extending from Pictou in northern NS, to eastern PEI, and the Magdalen Islands in QC. NO_2 levels in smaller communities on the north shores of Chaleur Bay and near the estuary of the St. Lawrence River, such as Baie-Comeau and Sept-Îles in QC, were higher than in their

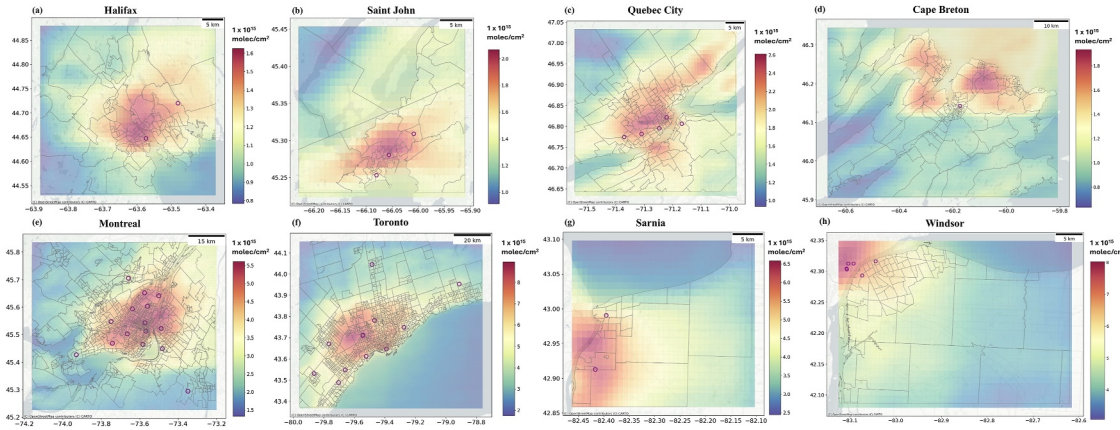

Figure 2. Annual mean of TEMPO (Tropospheric Emissions: Monitoring of Pollution) tropospheric nitrogen dioxide (NO_2) vertical column density (molec/cm^2) from 2023 September 1 to 2024 August 31 in eight selected Canadian municipalities in Atlantic Canada and the Quebec City-Windsor Corridor with high NO_2 pollution observed from Figure 1, including: (a) Halifax, (b) Saint John, (c) Quebec City, (d) Cape Breton, (e) Montreal, (f) Toronto, (g) Sarnia, (h) Windsor. The polygons indicate the boundary of census tracts, except for census dissemination areas in Cape Breton. The purple-colored circles indicate the locations of surface-level regulatory NO_2 monitoring stations. A spatial bilinear interpolation to 0.01° × 0.01° (1 km × 1 km) resolution was applied.

surrounding areas. During winter, NO_2 spread over the Gulf of St. Lawrence (Figure S1a in Supporting Information S1). In the QW Corridor (Figure 1b), two major pollution clusters were the Greater Toronto and the Detroit-Windsor metropolitan areas. Along with Port Huron-Sarnia, another transborder region to the north of Detroit-Windsor, these cities were persistent hotspots in all seasons. Moderately high annual mean NO_2 also occurred in Montreal, as well as Cleveland and Toledo on the south shore of Lake Erie. In winter, Quebec City experienced high NO_2, comparable to that in Montreal (Figure S1b in Supporting Information S1).

3.2. Intramunicipality NO_2 Pollution Patterns From TEMPO

Considering the spatial distribution of TEMPO annual mean observations (Figure 1), we selected eight municipalities with high NO_2 levels and a large population for further intraurban mapping: Halifax and Cape Breton in NS, Saint John in NB, Montreal and Quebec City in QC, Toronto, Windsor, and Sarnia in ON. For larger municipalities, including Halifax, Toronto, Montreal, and Quebec City, high-NO_2 clusters appeared in densely populated urban cores, where census tracts were more compact. High NO_2 in Windsor and Sarnia was concentrated in cross-border areas near the rivers (Figure 2). Cape Breton comprises several communities, and the highest pollution occurred on the northeastern coast.

We investigated tract-level NO_2 distributions for each selected municipality stratified by seasons, weekdays, and weekends. Based on Table 1, average good-quality observations in winter were much fewer than in other seasons, particularly for Montreal and Quebec City (below 1.5%). Regionally, Newfoundland and areas around the estuary of the St. Lawrence River (near Quebec City) had consistently lower fraction of retained pixels (Figure S2 in Supporting Information S1). Limited observations brought high uncertainties. In other words, results without sesaonal stratification are less representative of winter pollution. Still, given available observations, NO_2 levels in Toronto, Windsor, and Quebec City were noticeably higher in winter (Figure 3). Excluding winter, autumn is the season with the highest NO_2 for Halifax, Montreal, and Sarnia. Moreover, most municipalities maintained relatively low NO_2 in summer, except increases in Cape Breton during weekdays and in Sarnia.

Weekday-weekend differences were statistically significant for most selected municipalities and seasons, except for fall and winter in Saint John, winter and spring in Cape Breton and Quebec City, winter in Halifax, and summer in Sarnia (Table S1 in Supporting Information S1). Applying a filter of at least 60 weekday and 24 weekend good-quality observations in each census tract per season, we were unable to compare winter differences for five cities due to an insufficient number of observations (Halifax, Saint John, Quebec City, Montreal, Sarnia). For Toronto and Windsor, though statistically significant after filtering, winter differences became smaller in magnitudes. Furthermore, spatially resolved weekday-weekend PD indicated most areas, except for rural communities north of Saint John, had higher weekday concentrations (Figure S3 in Supporting Information S1). Saint John and Sarnia had a relatively smaller weekday-weekend difference (up to 20% against 40%–70% in other

Table 1
Seasonal Distribution of Good-quality Observations (Averaged Total Count of Pixels Retained Over All Pixel Locations and Its Percentage Over All Daytime Hours During That Season) of TEMPO (Tropospheric Emissions: Monitoring of Pollution) Tropospheric Nitrogen Dioxide (NO_2) Vertical Column Density (VCD) for the Eight Selected Municipalities

	Fall (September–November)				Winter (December–February)				Spring (March–May)				Summer (June–August)			
Population Center	Weekday (Mon–Fri)		Weekend (Sat–Sun)		Weekday (Mon–Fri)		Weekend (Sat–Sun)		Weekday (Mon–Fri)		Weekend (Sat–Sun)		Weekday (Mon–Fri)		Weekend (Sat–Sun)	
Cape Breton	120.4	17.9%	63.0	23.3%	22.5	3.9%	6.6	2.9%	196.7	24.5%	71.2	22.2%	204.4	27.8%	93.3	31.6%
Halifax	158.4	23.5%	55.9	20.7%	15.9	2.7%	12.9	5.6%	276.5	34.4%	70.3	21.9%	262.3	35.6%	91.6	31.0%
Saint John	157.6	23.4%	59.0	21.8%	46.3	8.0%	12.0	5.2%	277.2	34.5%	68.4	21.3%	275.7	37.5%	104.2	35.3%
Québec City	131.9	15.8%	52.8	15.8%	3.7	0.5%	0.6	0.2%	150.9	14.9%	36.3	9.0%	276.6	29.6%	116.1	31.0%
Montréal	167.9	20.2%	64.0	19.2%	8.1	1.1%	1.4	0.5%	205.5	20.3%	72.4	17.9%	261.7	28.0%	120.7	32.2%
Toronto	201.1	24.1%	85.4	25.7%	53.9	7.4%	21.7	7.5%	293.9	29.0%	69.5	17.2%	279.7	29.9%	124.4	33.2%
Sarnia	166.6	20.0%	75.8	22.8%	82.2	11.4%	13.1	4.5%	349.6	34.5%	92.6	22.9%	307.2	32.8%	144.6	38.5%
Windsor	167.9	20.2%	99.0	29.7%	84.2	11.6%	26.1	9.0%	335.7	33.1%	107.8	26.6%	296.2	31.6%	158.2	42.2%

Note. Each TEMPO image was screened with an effective cloud fraction below 20% and a snow-ice fraction below 5%. We defined seasons as (a) Fall: September–November 2023; (b) Winter: December 2023–February 2024; (c) Spring: March–May 2024; (d) Summer: June–August 2024.

municipalities). Weekday and weekend top-decile hotspot locations showed relatively large overlap in Toronto, Montreal, and Windsor, while they differed in Quebec City, spreading to the south (western Lévis) during weekdays but northeast during weekends.

Hourly population-weighted tract-averaged NO_2 VCDs for all eight selected municipalities are shown on Figure 4, stratified by weekdays and weekends. Consecutive hourly changes typically indicated when local NO_2 accumulated or was depleted (Figure S4 in Supporting Information S1). Weekend NO_2 in all eight municipalities and weekday NO_2 in the Atlantic provinces and QC peaked by 9 a.m. local time. Cities in ON attained weekday maxima 1 hr later at 10 a.m., with a major growth from 8 to 9 a.m. (11%–20%) followed by a sustaining increase in the subsequent hour (5%–6%). After the morning peak, NO_2 VCD gradually decreased and flattened during the afternoon and evening. Still, we observed local variabilities. For example, on weekdays, Sarnia maintained steady NO_2 levels from 9 a.m. until 6 p.m., as did Halifax until 2 p.m. Additionally, Sarnia had a strictly increasing trend after 1 p.m. on weekends. Occasionally, NO_2 levels rebounded in afternoon-to-evening hours, for instance, the weekday NO_2 in Halifax and Cape Breton after 6 p.m. Similarly, in the QW Corridor, besides the continuous NO_2

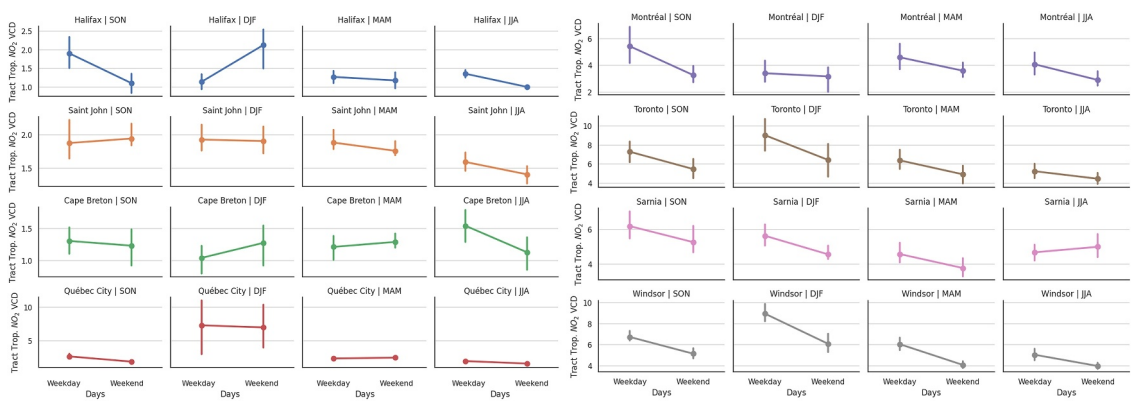

Figure 3. Seasonal variation in TEMPO (Tropospheric Emissions: Monitoring of Pollution) tropospheric nitrogen dioxide (NO_2) vertical column density (VCD) among the eight selected municipalities (from left to right, top to bottom: Halifax, Saint John, Cape Breton, Quebec City, Montreal, Toronto, Sarnia, Windsor) by seasons (columns, from left to right: SON, 2023 September 1 to November 30; DJF, 2023 December 1–2024 February 29; MAM, 2024 March 1 to May 31; JJA, 2024 June 1 to August 31). Winter months are excluded due to very limited good-quality observations in some areas. The census tract NO_2 VCDs (1×10^{15} molec/cm^2) are extracted by area-weighted mean (except using census dissemination areas for Cape Breton). The point represents the median NO_2 levels from all tracts, while each error bar extends to the upper and lower quartiles.

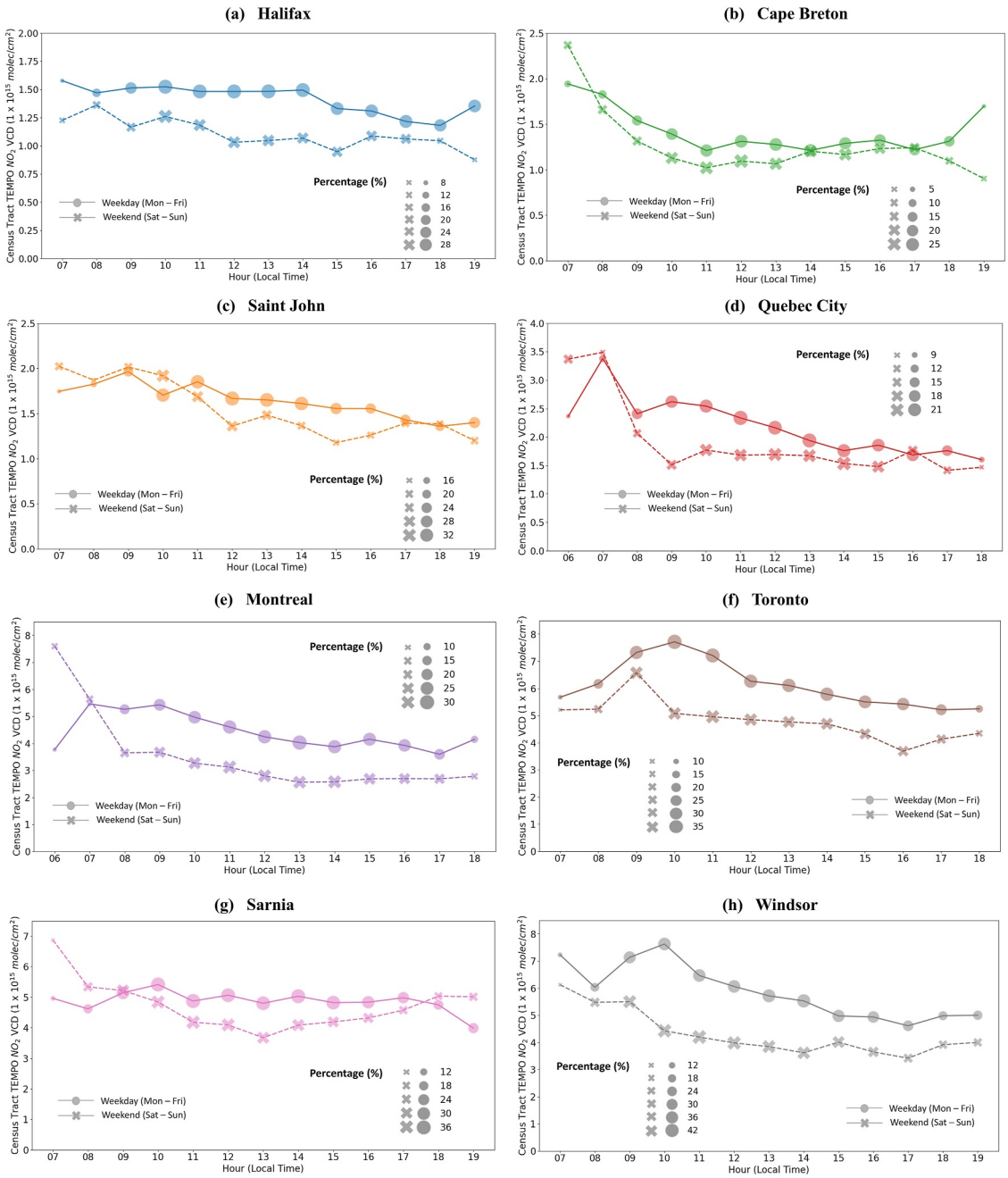

Figure 4. Diurnal hourly variation in TEMPO (Tropospheric Emissions: Monitoring of Pollution) tropospheric nitrogen dioxide (NO_2) vertical column density (VCD) from 2023 September 1 to 2024 August 31 among the eight selected municipalities: (a) Halifax, (b) Cape Breton, (c) Saint John, (d) Quebec City, (e) Montreal, (f) Toronto, (g) Sarnia, (h) Windsor, stratified by weekdays and weekends. To produce each hourly curve, we weighted census tract area-averaged NO_2 VCD by population (except using census dissemination areas for Cape Breton). The marker sizes are proportional to the percentage of observations retained from the quality screening for aggregation, averaged over all pixels in the corresponding municipality and hour.

rise in Sarnia, more than 10% weekend afternoon NO_2 increases were observed (Toronto: 4–5 p.m.; Windsor: 2–3 p.m. and 5–6 p.m.; Quebec City: 3–4 p.m.). Montreal experienced the greatest rise during weekday afternoons at 5–6 p.m. (+15.4%) among the QW corridor's municipalities. Further breakdown of diurnal patterns by seasons revealed local pollution characteristics in fall, spring, and summer (Figures S5–S7 in Supporting Information S1). Other than early morning peaks, drastic spikes were observed in spring on weekday noontime (11 a.m.–12 p.m.; +64.1%) for Cape Breton and weekend afternoon (3–4 p.m.) for Saint John (+60.2%), and in fall for Cape Breton (+59.1%).

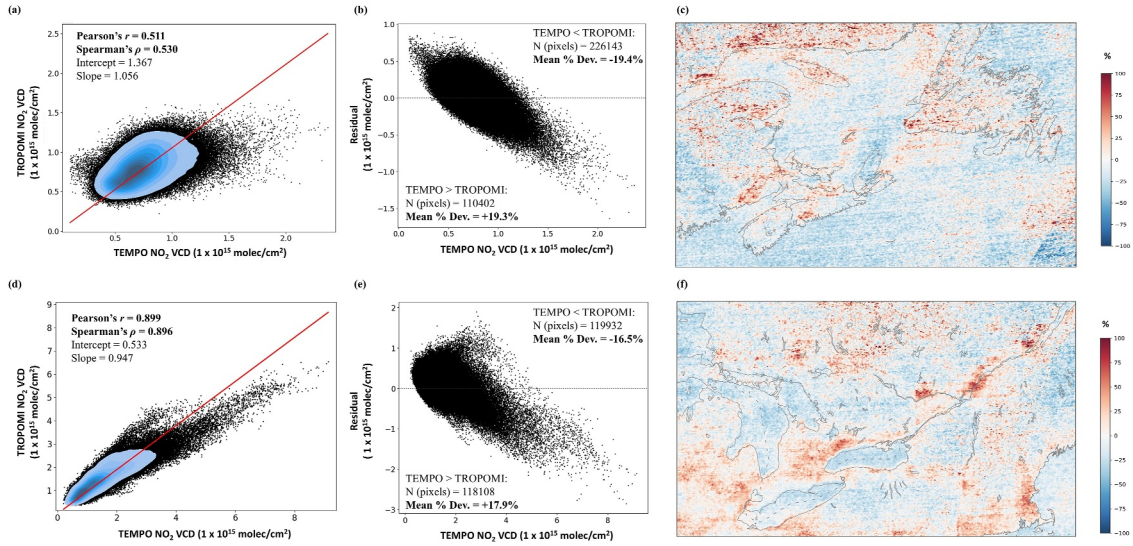

Figure 5. Comparison between TEMPO (Tropospheric Emissions: Monitoring of Pollution) and TROPOMI (Tropospheric Monitoring Instrument) tropospheric nitrogen dioxide (NO_2) vertical column densities (VCD), based on the paired images with scanning time differences within 15 min. The graph separates the outputs for (a–c) Atlantic Canada and (d–f) Quebec City-Windsor Corridor. The left column shows the regression plots with Pearson's and Spearman's correlation coefficients, intercepts, and slopes between the TEMPO and TROPOMI NO_2 VCD, the middle column indicates the residual plots (actual TROPOMI VCD against the estimated values from TEMPO VCD) of the regression, while the right column illustrates the spatial percentage differences: Δ = (TEMPO NO_2 – TROPOMI NO_2)/TROPOMI NO_2 * 100%, per each pixel.

3.3. Comparison Between TEMPO and TROPOMI Tropospheric NO_2

With the temporal matching (a 15-min window) and image filtering criteria (at least 50% of pixels retained considering scanning area overlap and quality), we extracted 39 and 45 TEMPO-TROPOMI paired images for the Atlantic and QW Corridor spatial extents accordingly from September 2023 to August 2024. The correlation coefficients between TEMPO and TROPOMI tropospheric NO_2 VCDs in the Atlantic region ($\rho = 0.53$; $r = 0.51$) were lower than those in the QW Corridor ($\rho = 0.90$; $r = 0.90$) (Figure 5). This is likely driven by the smaller dynamic range of observed values in Atlantic Canada compared to the QW Corridor, making random instrument variability more significantly impacting the correlational statistics. Comparing the pixelwise PD maps (Figures 5c and 5f) and the mean PD (MPD) over land cover classes based on annual leaf area index derived by the Moderate Resolution Imaging Spectroradiometer (MODIS) (Sulla-Menashe & Friedl, 2018) (Table S2 in Supporting Information S1), we found higher retrieved values from TEMPO than TROPOMI in urban and built-up areas (Atlantic Canada: +18.8%; QW Corridor: +25.8%). Additionally, TEMPO observed higher NO_2 in the sparsely populated rural areas in central-northern ON and QC, and around the Gulf of St. Lawrence. However, over water bodies, TEMPO detected lower NO_2 levels compared to TROPOMI (Atlantic Canada: −11.1%; QW Corridor: −12.1%). Averaged over pixels where TEMPO detected higher NO_2 VCD, the MPDs were 19.3% for Atlantic Canada and 17.9% for the QW Corridor. Conversely, on pixels with smaller TEMPO VCD, the magnitudes were 19.4% for Atlantic Canada and 16.5% for the QW Corridor. Overall, the absolute MPDs were 19.3% (Atlantic Canada) and 17.1% (QW Corridor), respectively. Moreover, we investigated the relationship between TEMPO-TROPOMI differences and land cover classes using linear regression adjusted with terrain height and surface albedo (Table S3 in Supporting Information S1). It reaffirmed that TEMPO-TROPOMI differences were positively biased on urban land cover but negatively biased over water with statistical significance. The magnitude of these biases were larger in the QW Corridor. Vegetation and terrain height had small impacts on the TEMPO-TROPOMI differences. Interestingly, surface albedo and TEMPO-TROPOMI differences were positively associated in Atlantic Canada ($\beta = 0.89$, CI: [0.87, 0.91]), but negatively associated in the QW Corridor ($\beta = -0.49$, CI: [−0.52, −0.45]).

3.4. Comparison Between TEMPO and Surface-Level NO_2

The two regions of interest showed dissimilar trends in TEMPO tropospheric NO_2 and AirNow surface-level measurements by monthly, weekly, day-of-week, and daytime hourly averages (Figure 6). The monitoring

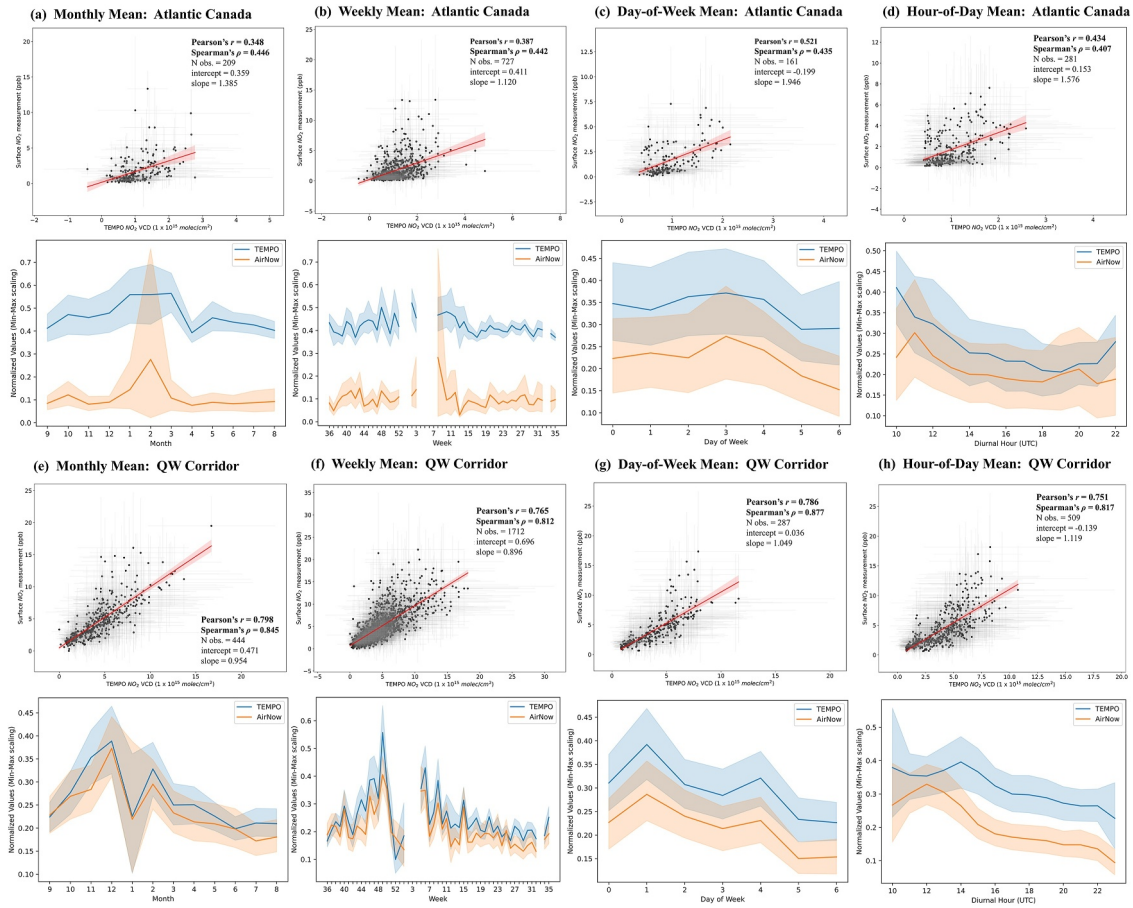

Figure 6. Comparison between spatiotemporally colocated TEMPO (Tropospheric Emissions: Monitoring of Pollution) tropospheric nitrogen dioxide (NO_2) vertical column density and surface NO_2 measurements from regulatory monitoring stations (data obtained through AirNow) in panels (a–d) Atlantic Canada and (e–h) Quebec City-Windsor Corridor. The four columns show comparisons at (from left to right): monthly mean (starting from September in 2023 to August in 2024); weekly mean (starting from the 36th week in 2023 to the 35th week in 2024); day-of-week mean (0 = Monday; 6 = Sunday); and diurnal hourly mean. For each column, the first row shows the regression plots with Pearson's and Spearman's correlation coefficients between TEMPO and surface NO_2, while due to their differences in physical units, the second row shows the normalized values of the two data sources varied by time.

data in the QW Corridor attained high correlations with TEMPO observations (ρ = 0.81–0.88; r = 0.75–0.80), while in Atlantic Canada, these were moderate (ρ = 0.41–0.45; r = 0.35–0.52). Moreover, the monthly and weekly averages of AirNow and TEMPO observations in the QW Corridor were more closely aligned with each other (Table S4 in Supporting Information S1). Observations for the first few weeks during January and February should be interpreted with caution due to very few good-quality observations from TEMPO. For the QW Corridor, column and surface NO_2 showed concurrent increases on Tuesday and Friday, with minima on weekends. Subdaily changes in surface NO_2 preceded TEMPO column NO_2 by approximately 2 hrs. For example, the peak in surface NO_2 at 12 p.m. UTC may correspond to that in TEMPO VCD at 2 p.m. UTC. Both measurements decreased during later hours. Surface NO_2 flattened at around 3–4 p.m. UTC, while column NO_2 flattened at 5 p.m. UTC. Residual patterns generally did not exhibit any clear trends but appeared slightly more dispersed at higher TEMPO VCD ranges for the daily and hourly comparison in the QW Corridor (Figure S8 in Supporting Information S1).

3.5. TEMPO-Derived Undermonitored NO_2 Hotspots

Eight population centers plus one First Nations reserve in Atlantic Canada had percentile ranks (PRs) of TEMPO's annual average greater than that of TROPOMI by a magnitude of 0.50 (i.e., 50%) (Table S5 in Supporting Information S1; Figure 7). These communities were mainly located on the north shores near the estuary of the St. Lawrence River and the Chaleur Bay in QC, with Channel-Port aux Basques at the southwestern corner of

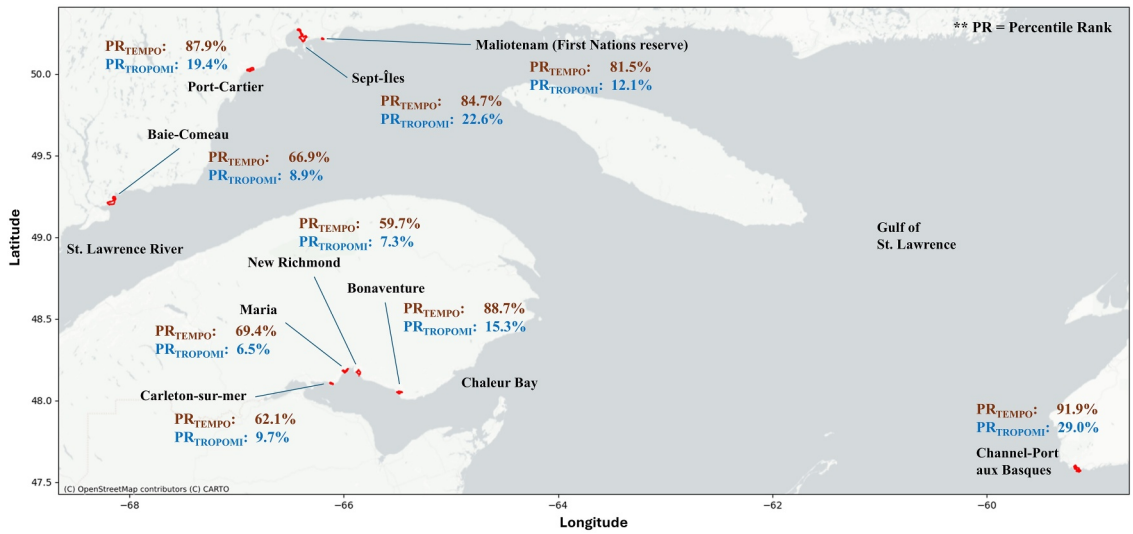

Figure 7. Population centers in the Atlantic Canada region with the difference in percentile ranks of tropospheric nitrogen dioxide (NO_2) vertical column density between TEMPO (Tropospheric Emissions: Monitoring of Pollution) and TROPOMI (Tropospheric Monitoring Instrument) greater than 0.5, that is, $PR_{TEMPO} - PR_{TROPOMI} > 0.5$, highlighted by red-colored polygons and annotated with community-specific labels on the map.

Newfoundland. For their NO_2 VCDs, seven out of nine were situated within TEMPO's upper-third (above the 67th percentile), while all fell within TROPOMI's bottom 30%. Figures S9 and S10 in Supporting Information S1 replicate the regional and municipality maps in Figures 1 and 2 using TROPOMI annual mean tropospheric NO_2 VCD. Moreover, the nearest ground-based monitoring stations were 50–300 km away from these population centers. TEMPO-TROPOMI PR differences from the spatiotemporally colocated data set of these coastal hot-spots were narrower than those from the annual averages, except for the First Nations reserve (Table S5 in Supporting Information S1). The consistent positive bias of TEMPO compared to TROPOMI in built-up areas (as identified in Section 3.3) might account for communities already having large spatiotemporally colocated PR differences (>40%). This might be attributed to instrumental specifications (e.g., orbits, viewing geometry, spectral coverage, etc.) and processing algorithms between TEMPO and TROPOMI. In contrast, we found communities with small TEMPO-TROPOMI PR differences or much lower TEMPO PRs in the spatiotemporally colocated data set (Port-Cartier, Carleton-sur-mer, Maria, Channel-Port aux Basques). Instrumental biases were unlikely to fully explain their large annual PR variations, implying that TEMPO's expanded daytime monitoring could help capture previously unobserved pollution. Understanding the causes of these differences is beyond the scope of our analysis but we encourage future research on this topic, especially in communities where TEMPO-TROPOMI PR differences are large.

Top-decile population centers derived from TEMPO's first-year NO_2 VCD agreed with TROPOMI observations in major populated and industrial cities while showing dissimilarities in suburban communities (Figure 8). Undermonitored communities are those with high NO_2 and no monitor in the neighborhood. For Cape Breton and Saint John (Figure 8a), monitors were primarily deployed in central areas (i.e., Sydney in Cape Breton and the port of Saint John). Three unmonitored communities near Sydney were located on the northern coast, which experienced higher TEMPO NO_2 levels (Figure 2). The northeastern suburbs of Saint John also had high NO_2, possibly impacted by emission sources from urban Saint John, but lacked surface monitoring to characterize the pollution levels and transport. TEMPO additionally identified Channel-Port aux Basques, NL and Cap-aux-Meules, QC as undermonitored communities. In the QW Corridor, a cluster of remote communities without nearby monitors to the south of Windsor had consistently high NO_2 VCD (Figure 8b). Meanwhile, TEMPO uniquely identified high pollution in Kitchener, Guelph, and Woodstock in Ontario, and more suburbs near northeast Montreal, but did not capture monitoring gaps in southern Niagara and Montreal, as compared to TROPOMI. Within the eight selected municipalities, TEMPO and TROPOMI showed the largest 98th percentile overlap in western Toronto and near Windsor (downtown Detroit) (Figure 9). In northeastern Cape Breton, TEMPO detected higher NO_2 over lands, against TROPOMI's NO_2 spread over marine areas. Similarly, the two instruments were less consistent around urban cores in Montreal, Quebec City, Saint John, and Halifax. In Sarnia,

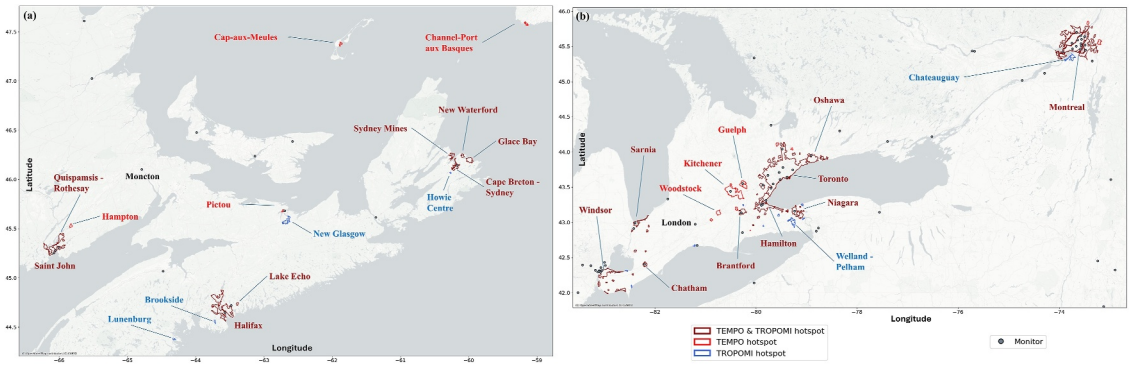

Figure 8. Population centers in (a) Atlantic Canada and (b) the Quebec City-Windsor Corridor identified as hotspots (exceeding the 90th percentile). The color classifications were defined based on the population center's area-weighted tropospheric nitrogen dioxide (NO_2) vertical column density annual averages from TEMPO (Tropospheric Emissions: Monitoring of Pollution) and TROPOMI (Tropospheric Monitoring Instrument) (from 2023 September 1 to 2024 August 31). Brown color indicates common hotspots from TEMPO and TROPOMI measurements during 2023–2024. Red and blue colors refer to those identified only from TEMPO and TROPOMI measurements, respectively. Additionally, the gray-colored points represent the current NO_2 regulatory monitoring locations.

TROPOMI detected hotspots closer to northern major residential zones, while TEMPO indicated top extremes in the southern areas.

Compared to using the annual average data set, hotspots mapped with the spatiotemporally colocated data set exhibited similar patterns regionally (agreement in most highly polluted cities with suburban variations), but less overlap for intraurban settings except the Detroit-Windsor area (Figures S11 and S12 in Supporting Information S1). Variations between TEMPO and TROPOMI hotspots in Figures 8 and 9 might result from a combination of factors, such as variations between TEMPO and TROPOMI retrievals by land characteristics (Section 3.3), difference in daytime temporal coverages of the two instruments, and potentially other unexplored variables. To further clarify intraurban NO_2 differences and strengthen the spatiotemporally colocated analysis, more data, such as ground-based measurements, are needed.

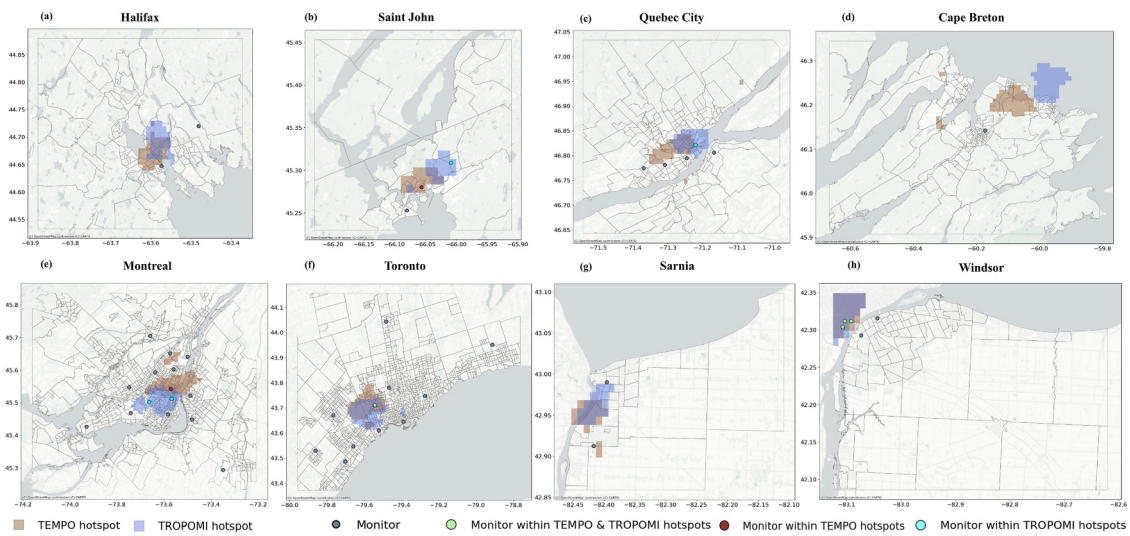

Figure 9. Intraurban hotspots (exceeding the 98th percentile) in the eight selected Canadian municipalities in Atlantic Canada and the Quebec City-Windsor Corridor with high nitrogen dioxide (NO_2) pollution observed from Figure 1, including: (a) Halifax, (b) Saint John, (c) Quebec City, (d) Cape Breton, (e) Montreal, (f) Toronto, (g) Sarnia, (h) Windsor. The color classifications were defined based on the annual mean tropospheric NO_2 vertical column density from TEMPO (Tropospheric Emissions: Monitoring of Pollution) and TROPOMI (Tropospheric Monitoring Instrument) from 2023 September 1 to 2024 August 31. Light-brown and slate-blue colored areas were derived from annual TEMPO and TROPOMI measurements, respectively. Gray-coloured points indicate current NO_2 regulatory monitoring locations. Correspondingly, light-green, dark-red and cyan colored points indicate whether the station is placed within the TEMPO and TROPOMI, TEMPO-specific, and TROPOMI-specific hotspots, respectively. The spatial resolution for intramunicipality mapping is 0.01° × 0.01° (1 km × 1 km).

4. Discussion

TEMPO advances high-resolution NO_2 monitoring, facilitating research on atmospheric processes, emissions, and health risks. In this study, we conducted an exploratory analysis on spatiotemporal patterns of first-year TEMPO tropospheric NO_2 and validated its agreement with TROPOMI and surface monitor data in eastern Canada. Specifically, we calculated population-weighted NO_2 concentrations, accounting for diurnal, seasonal, weekday-weekend, and community-level spatial variability. Compared to TROPOMI, which is limited to a once-per-day overpass at approximately 13:30 local time, TEMPO observed NO_2 during morning rush hours when traffic-related air pollution is more severe. TEMPO might also be more sensitive to local emissions in built-up areas. New TEMPO observations helped identify previously unrecognized high-pollution areas in eastern Canada that are currently not covered by the surface air pollution monitoring network. Comparing TEMPO NO_2 VCDs in monitored and unmonitored areas can support optimizing monitor site selection and better evaluate the monitor network's confidence to capture extreme pollution scenarios. Typically, established analysis relied on model-derived surface concentrations (Wang et al., 2024).

The eight municipalities with high TEMPO NO_2 levels were either densely populated urban centers or industrial hubs. Toronto and Montreal are the two largest metropolitan areas, each occupied by more than four million residents. Halifax is the most populous city in Atlantic Canada. Large cities have high traffic volumes and power consumption contributing to NO_2 emissions. Furthermore, most selected municipalities are close to marine transport routes. Saint John, Windsor, and Sarnia have heavy industry, such as chemical and oil refineries, pulp and paper mills, automotives etc., with the latter two situated on the U.S.-Canada border and impacted by transborder point and mobile source emissions.

Annually predominant southwesterly winds might be associated with observations among the three Atlantic port communities (Figure S13 in Supporting Information S1). The northeastern rural areas of Halifax (i.e., Lake Major) (Figure 2) and suburbs of Saint John (i.e., Quispamsis-Rothesay and Hampton) (Figure 8) were identified with high NO_2 from TEMPO. Despite being less populated, Cape Breton possesses three coal-fired or petroleum-based power plants. The prevailing winds might carry NO_2 emitted northeast leading to the emergence of TEMPO hotspots in New Waterford and Glace Bay, instead of its more populated center in Sydney, NS (Figure 2 and Figure S10 in Supporting Information S1), which illustrated a typical mismatch between observed hotspot and monitored locations (Figure 9d). Furthermore, northeastern transport of NO_2 emissions from Cape Breton across the Cabot Strait might impact southwestern Newfoundland (Channel-Port aux Basques) (Table S5 in Supporting Information S1). Interestingly, a year-round ferry service operates between Cape Breton and Channel-Port aux Basques. The ferry terminal is located on the northwestern coast of Cape Breton (Sydney Mines), where TEMPO observed high NO_2 but not TROPOMI. The scheduled routine departure at 11:45 a.m. and summer-specific departure at 5:30 p.m. also coincided with the annual noontime and summer weekday evening NO_2 rises in Cape Breton (Figure 4 and Figure S5 in Supporting Information S1). Moderately high NO_2 levels were also observed along ferry routes connecting Pictou in NS, eastern PEI, and Magdalen Islands in QC. Still, more evidence is required to confirm whether these were coincidences and quantify impacts from wind-driven NO_2 transport and shipping-related NO_2 emissions in Atlantic Canada.

Among communities with much higher TEMPO PRs (Figure 7; Table S5 in Supporting Information S1), Baie-Comeau and Sept-Îles are most populous stopover ports for transoceanic goods-carrying ships, with the aluminum processing industry (Adebayo et al., 2014; Ferrario et al., 2022). With iron ore mining activities, Sept-Îles is also a connection point for railway and truck transport. For communities by the Chaleur Bay, pollution sources are mainly found on the south shore in NB, including petroleum-fueled power and chemical processing plants (Fraser et al., 2011), which might contribute to cross-boundary pollution in QC. To our knowledge, public health outcomes associated with NO_2 exposure in these regions have not been well explored.

Differences between TEMPO and TROPOMI observations might also offer new insights into intraurban NO_2 pollution sources. TEMPO's 98th percentile specifically covered the North End neighborhood of Halifax, where major railroads, a shipyard, and cross-harbor bridges exist (Figure 9a). The harborside monitor is placed outside the highest polluted areas identified by both TEMPO and TROPOMI. In Quebec City, three monitoring stations are located south of the periphery of TEMPO's 98-percentile areas, unable to capture NO_2 extremes from high densities of railroads, highways, and an industrial park within that area (Figure 9c). For Montreal, TEMPO's high-NO_2 area was more north compared to those based on TROPOMI (Figure 2; Figure S10 in Supporting Information S1), coinciding with industrial zones near Longueuil and Montreal-Est (Figure 9e). In Sarnia, TEMPO

detected the highest NO_2 in the southwest, which is the city's manufacturing zone, known as the "Chemical Valley", accommodating 40% of Canada's chemical production (Atari et al., 2008) (Figures 2 and 9g). Local monitoring expansion is recommended around southern Sarnia to characterize exposure risks. In Toronto, the highest NO_2 occurred near the international airport and its proximal warehousing and distribution facilities (Figure 9f). Areas surrounding warehouses in the U.S. had 20% higher NO_2 VCD based on TROPOMI (Kerr et al., 2024), while similar investigations are lacking in Canada. Woodstock, an undermonitored hotspot identified specifically by TEMPO, is a manufacturing center for automotive assembling. In particular, Saint John and Montreal have regulatory monitors situated within TROPOMI's and TEMPO's 98th percentile areas, respectively (Figures 9b and 9e). Examining the AirNow surface NO_2 data at these monitors during the study period, we found that for Saint John, the monitor within TEMPO's 98th percentile recorded both higher daytime (7 a.m.–6 p.m.) and early afternoon overpass (1–2 p.m.) hourly averages (3.75 and 3.35 ppb) than the monitor within TROPOMI's 98th percentile (3.35 and 3.29 ppb). However, for Montreal, the daytime average was lower at the monitor within TEMPO's intraurban hotspots (7.11 ppb). Proximity to major highways (Autoroute 40 and Route 138) could lead to higher measurements from the other two surface monitors captured by TROPOMI (11.78 and 8.81 ppb).

The diurnal trend observed using TEMPO matches previous findings from in situ surface monitors or model simulations. In Halifax, nitrogen oxides (NOx) emissions based on measurements in 2017 also peaked in the early morning and then declined gradually (Mitchell et al., 2021). Ozone photochemistry might be an important factor accounting for seasonal NO_2 variations. TEMPO observed lower weekday NO_2 levels in Halifax and Cape Breton in spring than in summer (Figure S5 in Supporting Information S1). Prior research found a spring peak in ground-level ozone in NS (Mitchell et al., 2021), during which more NO_2 would be dissociated by sunlight. In contrast, ground-level ozone in the QW Corridor peaked in summer (Brook et al., 2014), when TEMPO observed minimum NO_2, except for Sarnia (Figure 3). Persistent release of pollutants from chemical production might account for Sarnia's distinct summer NO_2 diurnal patterns (Figure S5 in Supporting Information S1). Sarnia's afternoon increasing trend on weekends might align with the longer cross-border waiting time at the Blue Water Bridge (the U.S.-Canada crossing connected to Sarnia) during weekends after 2 p.m (Maoh et al., 2018), which leads to elevated emissions from trucks. Moreover, the weekday morning peak in Toronto during summer appeared late (11 a.m.). Studies suggested that in summer, photolysis causes a drop in the early morning NO_2, and conversion of nitrogen monoxide (NO) into NO_2 by ozone inflates satellite-observed NO_2 VCD in the late morning (Edwards et al., 2024).

TEMPO-TROPOMI and column-surface correlations in Atlantic Canada were significantly lower than in the QW Corridor (Figures 5 and 6). Background NO_2 in Atlantic Canada is lower than in the QW Corridor due to the lack of highly polluted large metropolitan areas like Toronto, Detroit-Windsor, and Montreal. Higher sensitivity and precision are required to discern smaller ranges of NO_2 levels. Situated at the eastern-edge granules and high latitudes, VCD in Atlantic Canada is subject to additional atmospheric corrections due to large SZA and VZA (Vanhellemont et al., 2014). Moreover, coarser spatial resolution at the edges of the FoR may lead to lower agreements with other observations due to oversmoothing. Analyzing SCD might be another research direction for further insights of NO_2 distributions. Moreover, TEMPO treated a pixel as either land or water and used the same wind-dependent climatological parameters to model water surface albedo (Nowlan et al., 2025), while TROPOMI considered mixed land cover pixels and sea ice conditions when adjusting for surface albedo (van Geffen et al., 2022). These differences might be associated with the greater contrast between urban and water retrievals from TEMPO compared to TROPOMI (Table S2 in Supporting Information S1), and different relationships between surface albedo and TEMPO-TROPOMI differences in the two regions (Table S3 in Supporting Information S1). Further research into the sensitivity of retrievals on surface albedo is needed.

This study has a few limitations that warrant future investigations. First, for Canada's high latitudes and cold weather, applying low cutoffs of cloud and snow fractions could mask a large proportion of pixels during winter months (Table 1). However, winter NO_2 pollution is usually more severe because of the reduced daylight suppressing NO_2 photolysis, shallower atmospheric boundary layer mixing, and increased fossil fuel combustion for residential or commercial consumptions (Brook et al., 2014; Mitchell et al., 2021). Recent research also found higher surface NO_2 during cloudy than clear-sky conditions (Goldberg et al., 2025). Imbalance in percentages of good-quality observations across seasons could bias spatial patterns when comparing annual aggregates regionally and locally. The summary statistics were potentially less representative of municipalities with fewer good-quality winter retrievals, particularly Quebec City and Montreal. Seasonal expansion of surface monitoring could fill data gaps and improve the estimation of surface exposure. Similarly, subdaily uncertainties are higher

during the sunrise and sunset hours (e.g., 7 a.m. and 6 p.m.) because AMF calculations depend on MODIS observations (overpass at 10:30 a.m. and 1:30 p.m.) (González Abad et al., 2024). High temporal-resolution surface monitoring could be targeted during these hours. Second, from our results, current TEMPO NO_2 retrievals appeared to have a larger contrast between built-up land and water compared to TROPOMI. Future studies may consider adjustments in processing algorithms or calibrating performance for offshore and rural NO_2 detection. We noted that TEMPO released an updated version (V04) in September 2025, while our analysis used V03 data. As update of TEMPO products is anticipated throughout its mission, similarly to other satellite-derived data products, using the most recent data could ensure the robustness of subsequent analyses. Third, we only analyzed TEMPO's first-year data, which might be prone to single-year anomalies. While our analysis is exploratory in nature, our findings still inform general spatiotemporal patterns, potential uncertainties, and how TEMPO-derived hotspots may differ from past understanding. As TEMPO has planned for a 15-yr operational lifetime (Zoogman et al., 2017), long-term analyses spanning multiple years of TEMPO measurements are necessary to assess diurnal variability and persistence of hotspots. This will also help evaluate TEMPO's biases against other satellite and ground-based instruments, ultimately adding the evidence needed for environmental policy evaluations and public health applications. Lastly, for surface measurements, AirNow only stores real-time data from NAPS monitors without validation. Validated data would be released 1 to 2 yrs later, and should be incorporated in future comparisons. Alternatively, the Pandora global network offers ground-based observations, though limited to Toronto and Windsor in eastern Canada (United Nations Environment Program Ozone Secretariat, 2024). Pandora provides columnar density with similar retrieval algorithms as satellite-based measurements, while NAPS monitors provide surface measurements based on chemiluminescence techniques and cavity attenuated phase shift spectroscopy, which might overestimate concentrations due to interference from reactive nitrates (Dunlea et al., 2007).

5. Conclusion

Our work summarized spatiotemporal patterns of tropospheric NO_2 in eastern Canada. Leveraging TEMPO's high-resolution data enabled us to examine diurnal variations, pinpoint population centers with previously unobserved NO_2 pollution, and assess intraurban hotspots not covered by the regulatory monitoring network. The findings on diurnal variations could potentially shape a more adaptable NO_2 control policy. For instance, by examining regions experiencing traffic congestion when peaks and rapid increases in NO_2 occurred, authorities might design or revamp transit and road systems considering emission mitigation. Our study makes an important first step toward better understanding NO_2 pollution and its association with emission sources, atmospheric transport, and health outcomes in eastern Canada. Next-step studies may focus on uncertainty of TEMPO observations, such as surface pollution in winter and variations by land characteristics.

Conflict of Interest

The authors declare no conflicts of interest relevant to this study.

Data Availability Statement

All data used in this manuscript's analyses are publicly available. TEMPO Level 3 tropospheric NO_2 VCD and its support data (provisional V03) were accessed from https://www.earthdata.nasa.gov/ and maintained by NASA's Atmospheric Science Data Center (DOI: https://doi.org/10.5067/IS-40e/TEMPO/NO2_L3.003) (Gorelick et al., 2017; NASA, 2024). TROPOMI Level 3 tropospheric NO_2 VCD was downloaded from the Google Earth Engine (GEE), collection "COPERNICUS/S5P/OFFL/L3_NO2", which is owned by the European Space Agency (European Space Agency, 2024). Similarly, the MODIS Type 3 (Annual Leaf Area Index) land use classification data were downloaded from GEE, collection "MODIS/061/MCD12Q1" (Sulla-Menashe & Friedl, 2018). Near real-time Canadian surface monitoring data were downloaded from AirNow through "PyRSIG" (GPL-3.0 license specified in the repository https://github.com/barronh/pyrsig), a Python package for the Remote Sensing Information Gateway maintained by U.S. EPA (https://epa.gov/rsig) (Henderson, 2025; US EPA, 2024). All codes and Jupyter Notebooks for the data extraction and visualization are implemented on Python (version $\geq$ 3.11) and made available in the repository: https://github.com/tksiu/tempo-no2-east-CA with MIT license (Siu, 2025). The processed data ready for loading, plotting, and generating outputs are deposited on Zenodo (Siu & Fong, 2025).

Acknowledgments
T.K. Siu and K.C. Fong were supported by funding from Dalhousie University and Research Nova Scotia (2022–2350). K.C. Fong also received support from the National Institute of Environmental Health Sciences of the National Institutes of Health under award number P20ES036775.

References

Achakulwisut, P., Brauer, M., Hystad, P., & Anenberg, S. C. (2019). Global, national, and urban burdens of paediatric asthma incidence attributable to ambient NO2 pollution: Estimates from global datasets. *The Lancet Planetary Health*, *3*(4), e166–e178. https://doi.org/10.1016/S2542-5196(19)30046-4

Adebayo, A. A., Zhan, A., Bailey, S. A., & MacIsaac, H. J. (2014). Domestic ships as a potential pathway of nonindigenous species from the saint Lawrence River to the Great Lakes. *Biological Invasions*, *16*(4), 793–801. https://doi.org/10.1007/s10530-013-0537-5

Anenberg, S. C., Mohegh, A., Goldberg, D. L., Kerr, G. H., Brauer, M., Burkart, K., et al. (2022). Long-term trends in urban NO2 concentrations and associated paediatric asthma incidence: Estimates from global datasets. *The Lancet Planetary Health*, *6*(1), e49–e58. https://doi.org/10.1016/S2542-5196(21)00255-2

Atari, D. O., Luginaah, I., Xu, X., & Fung, K. (2008). Spatial variability of ambient nitrogen dioxide and sulfur dioxide in Sarnia, "Chemical Valley," Ontario, Canada. *Journal of Toxicology and Environmental Health, Part A*, *71*(24), 1572–1581. https://doi.org/10.1080/15287390802414158

Brook, J. R., Burnett, R. T., Dann, T. F., Cakmak, S., Goldberg, M. S., Fan, X., & Wheeler, A. J. (2007). Further interpretation of the acute effect of nitrogen dioxide observed in Canadian time-series studies. *Journal of Exposure Science and Environmental Epidemiology*, *17*(S2), S36–S44. https://doi.org/10.1038/sj.jes.7500626

Brook, J. R., Dann, T. F., Galarneau, E., Herod, D., & Charland, J. P. (2014). The state of air quality in Canada: National patterns. *Air Quality Management: Canadian perspectives on a global issue*, 43–67. https://doi.org/10.1007/978-94-007-7557-2_3

Canadian Council of Ministers of the Environment (CCME). (2019). Ambient air monitoring and Quality Assurance/quality Control Guidelines. *National Air Pollution Surveillance Program*. Retrieved from https://ccme.ca/en/res/ambientairmonitoringandqa-qcguidelines_ensecure.pdf

Chance, K., Liu, X., Miller, C. C., Abad, G. G., Huang, G., Nowlan, C. R., et al. (2019). TEMPO Green Paper: Chemistry, physics, and meteorology experiments with the Tropospheric Emissions: Monitoring of pollution instrument. In *Sensors, Systems, and Next-Generation Satellites* (Vol. XXIII, pp. 56–67). https://doi.org/10.1117/12.2534883

Chance, K., Liu, X., Suleiman, R. M., Flittner, D. E., Al-Saadi, J., & Janz, S. J. (2013). Tropospheric emissions: Monitoring of pollution (TEMPO). In *Earth observing systems XVIII. Presented at the Earth observing systems XVIII, SPIE* (pp. 91–106). https://doi.org/10.1117/12.2024479

Dunlea, E. J., Herndon, S. C., Nelson, D. D., Volkamer, R. M., San Martini, F., Sheehy, P. M., et al. (2007). Evaluation of nitrogen dioxide chemiluminescence monitors in a polluted urban environment. *Atmospheric Chemistry and Physics*, *7*(10), 2691–2704. https://doi.org/10.5194/acp-7-2691-2007

Edwards, D. P., Martínez-Alonso, S., Jo, D. S., Ortega, I., Emmons, L. K., Orlando, J. J., et al. (2024). Quantifying the diurnal variation in atmospheric NO_2 from Geostationary Environment Monitoring Spectrometer (GEMS) observations. *Atmospheric Chemistry and Physics*, *24*(15), 8943–8961. https://doi.org/10.5194/acp-24-8943-2024

Environment and Climate Change Canada and United States Environmental Protection Agency. (2024). Review and assessment of the Canada-U. S. air quality agreement. Catalogue No.: En4-651/2024E-PDF, EC23244. Retrieved from https://www.epa.gov/system/files/documents/2024-03/review-and-assessment-of-the-canada-us-aqa-508-compliance.pdf. accessed 19 February 2025.

European Space Agency. (2024). Sentinel-5P OFFL NO2: Offline sulfur dioxide | Earth engine data catalog [Dataset]. *Google for Developers*. Retrieved from https://developers.google.com/earth-engine/datasets/catalog/COPERNICUS_S5P_OFFL_L3_NO2

Ferrario, F., Araújo, C. A. S., Bélanger, S., Bourgault, D., Carrière, J., Carrier-Belleau, C., et al. (2022). Holistic environmental monitoring in ports as an opportunity to advance sustainable development, marine science, and social inclusiveness. *Elementa: Science of the Anthropocene*, *10*(1), 00061. https://doi.org/10.1525/elementa.2021.00061

Fraser, M., Surette, C., & Vaillancourt, C. (2011). Spatial and temporal distribution of heavy metal concentrations in mussels (Mytilus edulis) from the Baie des Chaleurs, New Brunswick, Canada. *Marine Pollution Bulletin*, *62*(6), 1345–1351. https://doi.org/10.1016/j.marpolbul.2011.03.036

Gan, W. Q., FitzGerald, J. M., Carlsten, C., Sadatsafavi, M., & Brauer, M. (2013). Associations of ambient air pollution with chronic obstructive pulmonary disease hospitalization and mortality. *American Journal of Respiratory and Critical Care Medicine*, *187*(7), 721–727. https://doi.org/10.1164/rccm.201211-2004OC

Geddes, J. A., Martin, R. V., Bucsela, E. J., McLinden, C. A., & Cunningham, D. J. M. (2018). Stratosphere–troposphere separation of nitrogen dioxide columns from the TEMPO geostationary satellite instrument. *Atmospheric Measurement Techniques*, *11*, 6271–6287. https://doi.org/10.5194/amt-11-6271-2018

Goldberg, D. L., Nawaz, M. O., Lyu, C., He, J., Carlton, A. G., Kondragunta, S., & Anenberg, S. C. (2025). NO_2 concentration differences under clear versus cloudy skies and implications for applications of satellite measurements. *EGUsphere*, 1–23. https://doi.org/10.5194/egusphere-2025-1350

González Abad, G., Nowlan, C. R., Wang, H., Chong, H., Houck, J., Liu, X., & Chance, K. (2024). Trace Gas and Cloud Level 2 and 3 Data Products: User Guide. *Tropospheric Emissions: Monitoring of Pollution (TEMPO) Project*. Retrieved from https://asdc.larc.nasa.gov/documents/tempo/guide/TEMPO_Level-2-3_trace_gas_clouds_user_guide_V1.0.pdf

Gorelick, N., Hancher, M., Dixon, M., Ilyushchenko, S., Thau, D., & Moore, R. (2017). Google Earth Engine: Planetary-scale geospatial analysis for everyone. *Remote Sensing of Environment, Big Remotely Sensed Data: tools, applications and experiences*, *202*, 18–27. https://doi.org/10.1016/j.rse.2017.06.031

Henderson, B. H. (2025). Barronh/pyrsig, Python interface to RSIG Web API (Version 0.10.0). [Software]. https://barronh.github.io/pyrsig/

Hoff, R. M., & Christopher, S. A. (2009). Remote sensing of particulate pollution from space: Have we reached the promised land? *Journal of the Air & Waste Management Association*, *59*(6), 645–675. https://doi.org/10.3155/1047-3289.59.6.645

Holloway, T., Bratburd, J. R., Fiore, A. M., Kerr, G. H., & Mao, J. (2025). Satellite data to support air quality assessment and management. *Journal of the Air & Waste Management Association*, *75*(6), 429–463. https://doi.org/10.1080/10962247.2025.2484153

Holloway, T., Miller, D., Anenberg, S., Diao, M., Duncan, B., Fiore, A. M., et al. (2021). Satellite monitoring for air quality and health. *Annual Review of Biomedical Data Science*, *4*(1), 417–447. https://doi.org/10.1146/annurev-biodatasci-110920-093120

Kerr, G. H., Meyer, M., Goldberg, D. L., Miller, J., & Anenberg, S. C. (2024). Air pollution impacts from warehousing in the United States uncovered with satellite data. *Nature Communications*, *15*(1), 6006. https://doi.org/10.1038/s41467-024-50000-0

Lévesque, É. (2010). Ontario-Quebec trade corridor and Continental gateway. Presentation on: Best practices in urban transportation planning. *2010 Annual Conference Transportation Association of Canada*. http://conf.tac-atc.ca/english/resourcecentre/readingroom/conference/conf2010/docs/b1/levesque-e.pdf

Liu, X., Chance, K., Chong, H., Davis, J., Fitzmaurice, J., Gonzalez Abad, G., et al. and the TEMPO team (2025). A new era of air quality monitoring from space over North America with TEMPO: Early years in orbit. *EGU General Assembly*, EGU25–14388. https://doi.org/10.5194/egusphere-egu25-14388

Manisalidis, I., Stavropoulou, E., Stavropoulos, A., & Bezirtzoglou, E. (2020). Environmental and health impacts of air pollution: A review. *Frontiers in Public Health*, *8*, 14. https://doi.org/10.3389/fpubh.2020.00014

Maoh, H., Gingerich, K., Husein, R., & Anderson, W. (2018). Examining the variability of crossing times for Canadian trucks at the three major Canada–U.S. border crossings. *The Professional Geographer*, *70*(3), 350–362. https://doi.org/10.1080/00330124.2017.1385401

Meng, Z., & Comer, B. (2022). Great Lakes-St. Lawrence Seaway ship emissions inventory, 2019. *The Brief: International Council on Clean Transportation*. https://theicct.org/wp-content/uploads/2022/03/Great-Lakes-emissions_final.pdf

Mills, I. C., Atkinson, R. W., Kang, S., Walton, H., & Anderson, H. R. (2015). Quantitative systematic review of the associations between short-term exposure to nitrogen dioxide and mortality and hospital admissions. *BMJ Open*, *5*, e006946. https://doi.org/10.1136/bmjopen-2014-006946

Mitchell, M., Wiacek, A., & Ashpole, I. (2021). Surface ozone in the North American pollution outflow region of Nova Scotia: Long-term analysis of surface concentrations, precursor emissions and long-range transport influence. *Atmospheric Environment*, *261*, 118536. https://doi.org/10.1016/j.atmosenv.2021.118536

Naeger, A. R., Judd, L., Liu, X., Chance, K., Nowlan, C. R., & Gonzalez Abad, G. (2024). Delivering revolutionary satellite data with NASA's tropospheric emissions: Monitoring of pollution (TEMPO) Mission. *EM Plus Q1*, 6–12. 2024.https://www.researchgate.net/publication/381255245

Naeger, A. R., Newchurch, M. J., Moore, T., Chance, K., Liu, X., Alexander, S., et al. (2021). Revolutionary air-pollution applications from future tropospheric emissions: Monitoring of pollution (TEMPO) observations. *Bulletin of the American Meteorological Society*, *102*(9), 1735–1741. https://doi.org/10.1175/BAMS-D-21-0050.1

NASA. (2024). NASA/LARC/SD/ASDC, TEMPO gridded NO2 tropospheric and stratospheric columns [Dataset]. *V03 (PROVISIONAL)*. https://doi.org/10.5067/IS-40e/TEMPO/NO2_L3.003

Nowlan, C. R., González Abad, G., Liu, X., Wang, H., & Chance, K. (2025). TEMPO Nitrogen Dioxide Retrieval Algorithm theoretical basis document. Retrieved from https://asdc.larc.nasa.gov/documents/tempo/ATBD_TEMPO_NO2.pdf. accessed 20 February 2025.

Palmer, P. I., Jacob, D. J., Chance, K., Martin, R. V., Spurr, R. J. D., Kurosu, T. P., et al. (2001). Air mass factor formulation for spectroscopic measurements from satellites: Application to formaldehyde retrievals from the Global Ozone Monitoring Experiment. *Journal of Geophysical Research*, *106*(D13), 14539–14550. https://doi.org/10.1029/2000JD900772

Pan, J. J., & Chang, C. I. (1992). Destriping of Landsat MSS images by filtering techniques. *Photogrammetric Engineering & Remote Sensing*, *58*, 1417–1423.

Parajuli, R. P., Shin, H. H., Maquiling, A., & Smith-Doiron, M. (2021). Multi-pollutant urban study on acute respiratory hospitalization and mortality attributable to ambient air pollution in Canada for 2001–2012. *Atmospheric Pollution Research*, *12*, 101234. https://doi.org/10.1016/j.apr.2021.101234

Siu, T. (2025). tksiu/tempo-no2-east-CA: V1.0.1 [Software]. *Zenodo*. https://doi.org/10.5281/zenodo.17439606

Siu, T., & Fong, K. (2025). Processed TEMPO and TROPOMI tropospheric NO2 vertical column density in eastern Canada (Ontario, Quebec, Atlantic) from 2023 September to 2024 August [Dataset]. *Zenodo*. https://doi.org/10.5281/zenodo.17436052

Statistics Canada. (2012). Human Activity and the Environment: Waste management in Canada. Catalogue no. 16-201-X. Retrieved from https://www150.statcan.gc.ca/n1/pub/16-201-x/16-201-x2012000-eng.pdf

Statistics Canada (2023). Census profile. 2021 census of population. *Statistics Canada Catalogue number 98-316-X2021001. Ottawa. Released.* Retrieved from https://www12.statcan.gc.ca/census-recensement/2021/dp-pd/prof/index.cfm?Lang=E

Stevens, R., Poterlot, C., Trieu, N., Alejandro Rodriguez, H., & L. Hayes, P. (2024). Transboundary transport of air pollution in eastern Canada. *Environmental Science: Advances*, *3*, 448–469. https://doi.org/10.1039/D3VA00307H

S[&]T, The Netherlands. (2024). HARP manual — HARP 1.23 documentation. Retrieved from https://stcorp.github.io/harp/doc/html/index.html

Sulla-Menashe, D., & Friedl, M. A. (2018). *User guide to collection 6 MODIS land cover (MCD12Q1 and MCD12C1) product* (Vol. 1, p. 18). Usgs. Retrieved from https://lpdaac.usgs.gov/documents/101/MCD12_User_Guide_V6.pdf

United Nations Environment Program Ozone Secretariat. (2024). Canadian national report for the 12th WMO/UNEP ozone research managers meeting Geneva, 24-26 April 2024. Retrieved from https://ozone.unep.org/system/files/documents/ORM12-Canada-national%20report.pdf

US EPA (2024). Remote sensing information gateway. Retrieved from https://www.epa.gov/hesc/remote-sensing-information-gateway

van Geffen, J. H. G. M., Eskes, H. J., Boersma, K. F., & Veefkind, J. P. (2022). TROPOMI ATBD of the total and tropospheric NO2 data products. issue 2.4.0. S5P-KNMI-L2-0005-RP. Retrieved from https://asdc.larc.nasa.gov/documents/tempo/ATBD_TEMPO_NO2.pdf

Vanhellemont, Q., Neukermans, G., & Ruddick, K. (2014). Synergy between polar-orbiting and geostationary sensors: Remote sensing of the ocean at high spatial and high temporal resolution. *Remote Sensing of Environment, Liege Colloquium Special Issue: Remote sensing of ocean colour, temperature and salinity*, *146*, 49–62. https://doi.org/10.1016/j.rse.2013.03.035

Wang, Y., Marshall, J. D., & Apte, J. S. (2024). U.S. ambient air monitoring network has inadequate coverage under new PM2.5 Standard. *Environmental Science & Technology Letters*, *11*, 1220–1226. https://doi.org/10.1021/acs.estlett.4c00605

White, J. E., Wayland, R. A., Dye, T. S., & Chan, A. C. (2004). AIRNow air quality notification and forecasting system. In *Beijing international environment forum* (pp. 14–15). Retrieved from https://wiki.esipfed.org/w/images/2/25/AIRNow_Program.pdf

Zoogman, P., Liu, X., Suleiman, R. M., Pennington, W. F., Flittner, D. E., Al-Saadi, J. A., et al. (2017). Tropospheric emissions: Monitoring of pollution (TEMPO). *Journal of Quantitative Spectroscopy and Radiative Transfer*, *186*, 17–39. https://doi.org/10.1016/j.jqsrt.2016.05.008